Molecular Mechanisms for the Reaction Between (•)OH Radicals and Proline: Insights on the Role as ROS Scavenger in Plant Stress.

ARTICLE *in* THE JOURNAL OF PHYSICAL CHEMISTRY B · DECEMBER 2013

Impact Factor: 3.3 · DOI: 10.1021/jp407773u · Source: PubMed

4 AUTHORS, INCLUDING:

Santiago Signorelli
University of Western Australia
11 PUBLICATIONS **83** CITATIONS
SEE PROFILE

Elena Laura Coitiño
University of the Republic, Uruguay
45 PUBLICATIONS **701** CITATIONS
SEE PROFILE

Omar Borsani
University of the Republic, Uruguay
44 PUBLICATIONS **2,119** CITATIONS
SEE PROFILE

THE JOURNAL OF PHYSICAL CHEMISTRY B

Article

pubs.acs.org/JPCB

Molecular Mechanisms for the Reaction Between •OH Radicals and Proline: Insights on the Role as Reactive Oxygen Species Scavenger in Plant Stress

Santiago Signorelli,*[,†] E. Laura Coitiño,*[,‡] Omar Borsani,[†] and Jorge Monza[†]

[†]Laboratorio de Bioquímica, Departamento de Biología Vegetal, Facultad de Agronomía, Universidad de la República, Av. E. Garzón 780, CP 12900 Montevideo, Uruguay

[‡]Laboratorio de Química Teórica y Computacional (LQTC), Instituto de Química Biológica, Facultad de Ciencias, Universidad de la República, Iguá 4225, Montevideo 11400, Uruguay

Supporting Information

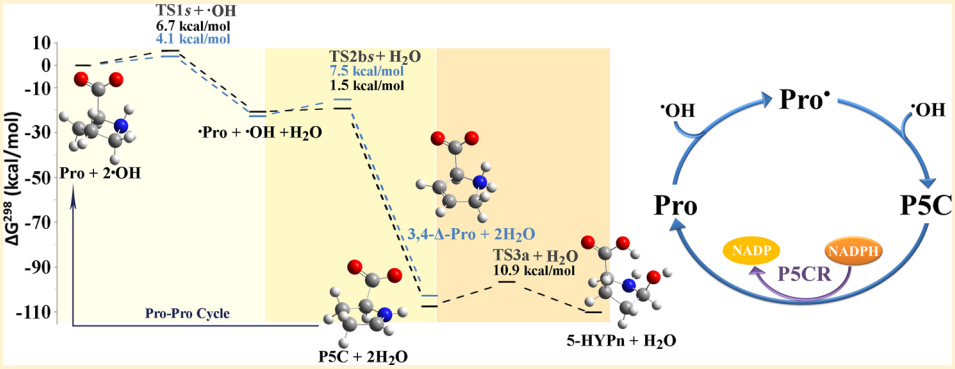

ABSTRACT: The accumulation of proline (**Pro**) and overproduction of reactive oxygen species (ROS) by plants exposed to stress is well-documented. In vitro assays show that enzyme inactivation by hydroxyl radicals (•OH) can be avoided in the presence of **Pro**, suggesting this amino acid might act as a •OH scavenger. Although production of hydroxyproline (**Hyp**) has been hypothesized in connection with such antioxidant activity, no evidence on the detailed mechanism of scavenging has been reported. To elucidate whether and how **Hyp** might be produced, we used density functional theory calculations coupled to a polarizable continuum model to explore 27 reaction channels including H-abstraction by •OH and •OH/H_2O addition. The structure and energetics of stable species and transition states for each reaction channel were characterized at the PCM-(U)M06/6-31G(d,p) level in aqueous solution. Evidence is found for a main pathway in which **Pro** scavenges •OH by successive H-abstractions ($\Delta G^{\ddagger,298}$ = 4.1 and 7.5 kcal mol^{-1}) to yield **3,4-Δ-Pro**. A companion pathway with low barriers yielding Δ^1-pyrroline-5-carboxylate (**P5C**) is also supported, linking with **5-Hyp** through hydration. However, this connection remains unlikely in stressed plants because **P5C** would be efficiently recycled to **Pro** (contributing to its accumulation) by **P5C** reductase, hypothesis coined here as the "Pro-Pro cycle".

1. INTRODUCTION

When plants are exposed to biotic and/or abiotic stress, damage on cellular components (proteins, lipids, carbohydrates, and DNA) is induced as a result of the overproduction of reactive oxygen species (ROS) such as hydrogen peroxide (H_2O_2), superoxide anion ($O_2^{\bullet-}$), and hydroxyl radicals (•OH).[1−3] The latter is the most reactive species among ROS and can be generated in vivo both by Fenton's reaction or through homolysis of H_2O_2 under UV radiation, to which plants are highly exposed. Hydrogen abstraction, addition, and electron-transfer processes are the most common reaction channels for •OH, leading to new radicals or closed-shell species with lower reactivity.[4] Cellular defense against ROS involves both enzymatic and nonenzymatic antioxidant systems.[1−3,5] Superoxide dismutase, catalase, and peroxidase are representative enzymes whose induction is associated to stress acclimation.[5] Glutathione, ascorbic acid, and tocopherols are common examples of nonenzymatic systems involved in the antioxidant plant's defense,[1] a category to which some authors also ascribe proline.[6]

Accumulation of proline up to 100 times the normal level in stressed plants has been a well-known fact for more than 40 years,[7] reaching cytosol concentrations of 120−230 mM (see Ashraf and Foolad[8] and references therein). Accumulation by de novo synthesis observed under drought and high salinity conditions, UV/vis irradiation, oxidative stress, in presence of heavy metals, or as a response to different kinds of biotic stresses[9]

Received: August 3, 2013
Revised: December 11, 2013
Published: December 14, 2013

   dx.doi.org/10.1021/jp407773u | J. Phys. Chem. B 2014, 118, 37−47

has been reported to be a feature shared by a wide variety of organisms including bacteria, fungi, and plants.[10] Whereas some authors have proposed that proline could act as a compatible osmolyte,[11,12] others hypothesized it might act as a non-enzymatic antioxidant[6] maintaining the redox potential in the cell[13] and scavenging ROS such as $^{\bullet}OH$[14,15] and singlet oxygen ($^1O_2$)[16] (albeit for the latter some of us recently showed proline does not quench singlet oxygen[17]). Other authors also proposed alternative roles for the species, such as stabilizing protein structure[18] or acting as C/N storage.[19] Early in 1989, Sminorff and Cumbes showed that enzyme inactivation by $^{\bullet}OH$ can be avoided in vitro in the presence of **Pro**, proposing the molecule might act as a $^{\bullet}OH$ scavenger.[14] In vivo assays conducted by Jain et al. on callus subjected to saline stress showed its accumulation decreases lipid peroxidation, suggesting that proline might contribute to the antioxidant defense.[20] Moreover, indirect evidence also emerges in comparing oxidative damage under stress on genetically engineered plants containing transgenes for production of proline; whereas transgenics with increased accumulation under saline conditions suffer less oxidative damage,[21,22] those unable to accumulate proline exhibit a significantly lower tolerance to stress compared to wild-type plants.[23,24]

Although the concept of proline acting as an antioxidant has been frequently referenced during the last 20 years (more than 600 citations of the original article by Smirnoff and Cumbes[14]), proposals on a detailed mechanism of its reaction with $^{\bullet}OH$ and the physicochemical features of the species involved along the possible reaction paths are still lacking. The absence of experimental evidence is possibly due to the high reactivity of the radical, a feature that makes use of experimental approaches difficult. The only suggestion currently advanced is that proline could react with $^{\bullet}OH$ mainly forming 5-hydroxyproline (**5-Hyp**),[15] but no clear evidence of the presence of this molecule under plant stress has been reported yet. In this scenario, computational modeling by quantum methods such as those based on the density functional theory (DFT) appears as a very valuable approach to explore the features of possible pathways with atomic and electronic levels of detail.

Ab initio post-Hartree−Fock and DFT calculations have already been applied with success to characterize structural features of the most stable isomers both for neutral proline in vacuo[25−29] and for zwitterionic/ionized proline in solution.[30−35] Four stable isomers displaying internal hydrogen bond (HB) between the −C(=O)OH and −N(H) moieties have been found in the gas phase, resulting from the combination of two possible N···H−O/N−H···O=C HB patterns with the C^{γ} *endo*- and *exo*-like puckering conformations relative to −COOH.[29] The main species in aqueous solution at near-physiological pH corresponds to the zwitterionic form. According to DFT/PCM calculations[31] the structure also displays an internal $CO_2^{-}\cdots H-NH^{+}$ interaction with a HB distance of 1.85 Å (1.91 Å in a second ring-puckered conformer) which is lengthened by 0.05 Å when three explicit waters are included in the model. These findings are consistent with neutron scattering and Raman experiments pointing out hydration favors a transition from neutral to zwitterionic species through strong interactions with water molecules.[36] FTIR data suggests there are at most three HBs per molecule, with no evidence for extended HB networking.[37] Two ring-puckering down/up conformations of the zwitterion, respectively corresponding to C^{γ} and the C=O group lying on the same/opposite side of the $C^{\alpha}-N-C^{\delta}$ plane were also found to be shallow minima on the molecular potential energy surface (PES). A barrier of 1.72−2.08 kcal mol^{-1} (hysteretic dependence of energy on the angle was found) for interconverting them via ring twists was reported at the B3LYP/6-311++G** COSMO-(H_2O) level by Bouř and co-workers,[33] suggesting both conformers would be present under physiological conditions. Approximately equal Boltzmann populations are predicted at 298−300 K and pH 6.8−7.2 from several NMR-based analyses and computational modeling, with the down (C^{γ} *endo*) conformer slightly preferred in terms of energy (<1 kcal mol^{-1}).[32−34,38] Ionization state, conformational preferences, and HB are all elements that must be considered in properly describing how conditions resembling those in the cell of a stressed plant may modulate the reactivity of the amino acid and the susceptibility of each of the target sites toward radical attack (i.e., captodative effects[39] stabilizing C^{α} radicals are not present in a zwitterion).

Despite a considerable body of information has been built on studies of the primary steps for the reaction of $^{\bullet}OH$ with amino acids in peptides and proteins,[40−53] quite less is known at a detailed level for the H-abstraction from *free* amino acids, with a series of studies available in gas phase[54−57] and in aqueous solution.[58−64] These reactions are fast, in the near-diffusion limit, with an overall rate constant of 6.5×10^8 M^{-1} s^{-1} determined for proline in aqueous solution at pH 6.8 and 298.15 K.[58] The fate of the process over free amino acids is determined by the strength of the C−H bonds targeted by $^{\bullet}OH$ and the stability of the radicals thus produced as the main controlling factors[42] combined with the outcome of a subtle balance among attractive and repulsive interactions the approaching hydroxyl radical establishes with the carboxylate moiety.[47,49,65] Any possible H-atom abstraction is expected to be strongly exergonic, because the O−H bond dissociation energy (BDE) in H_2O (ca. 119.3−118.8 kcal mol^{-1})[66,67] is higher than the BDEs for any C−H bond in proline zwitterion. Moore and Julian[68] coupled DFT calculations with isodesmic reactions to evaluate on an equal footing BDEs for X−H bonds (X = C, N, O, S) along the 20 common amino acids as being in a peptide backbone. Values of 84.3, 98.7, 99.1, and 93.9 ± 2.4 kcal mol^{-1} were found for the C−H homolytic cleavage at the α, β, γ, and δ sites, respectively, in *N*-acetylproline amide. A significant increase in the C^{α}−H BDE is expected for free proline in the zwitterionic form, as replacement at the N-terminus of the acetyl cap by an amine and its protonation are opposite effects that globally destabilize radicals both at the backbone C^{α} and (to a smaller extent) at the adjacent side-chain carbon. Assuming transferability across amino acids for the overall magnitude of these effects (+12.8 kcal mol^{-1} for alanine[68]), a final value of 97.1 kcal mol^{-1} might in principle be expected for the C^{α} position in free proline, leading to the following ordering of C−H BDEs: δ (C5) < α (C2) < β (C3) ≅ γ (C4), following now the numbering shown in Scheme I. However, only side-chain radicals were found in an early ESR characterization of the spin-trapped free radicals produced by reaction of $^{\bullet}OH$ with proline in aqueous solution.[60] From that study, Rustgi et al.[60] inferred that (as other authors have also done[40,42]) the short-lived species with the unpaired electron at C5 would be the most stable product for the primary step of the reaction. Although some controversies are still open on the relative reactivity toward H-atom abstraction at each site of the side-chain,[61] those first findings excluding C2 proline radicals as an outcome of the reaction with $^{\bullet}OH$ were further confirmed by more recent mass spectrometry[69] and $^2H/^1H$ NMR[47,61] studies. On the basis of some of that evidence, Matysik et al. hypothesized that **5-Hyp** could be the main product of the $^{\bullet}OH$ scavenging activity of proline.[15] Here we

dx.doi.org/10.1021/jp407773u | J. Phys. Chem. B 2014, 118, 37−47

Scheme I. Possible Reaction Pathways Explored in the Attempt to Explain Formation of Hyp through •OH Scavenging by the Zwitterionic Species in Aqueous Solution[a]

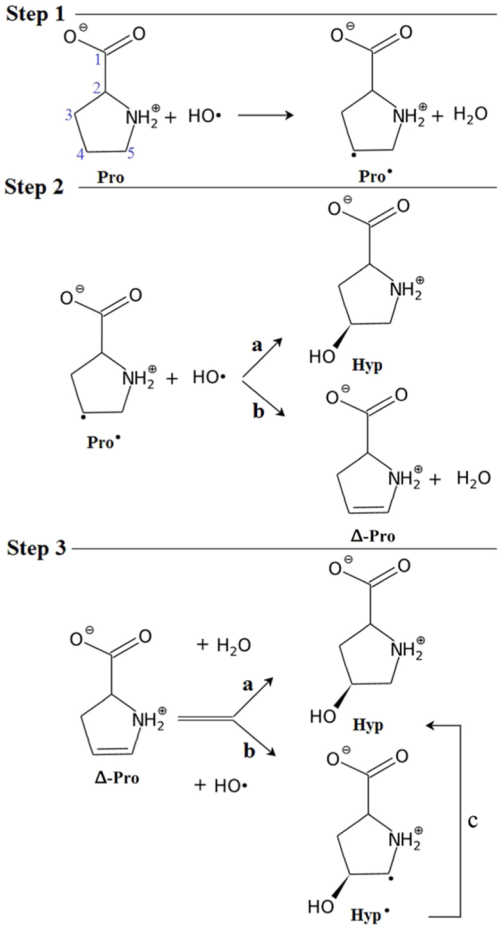

[a]Atom numbering scheme is depicted over **Pro** in blue characters.

intend to shed light on these controversial aspects relying on computational models capable to find evidence, if any, in support for such scavenger activity by exploring the features of feasible reaction channels connected with the formation of hydroxyproline.

2. MATERIAL MODELS AND COMPUTATIONAL METHODS

2.1. Molecular Systems. Several reaction pathways starting with H-atom abstractions by •OH from the most stable conformer of the zwitterionic form of proline in aqueous solution (**Pro** hereafter) were extensively explored. A comparison with the features of the neutral species displaying an internal HB as conducted at the same level of theory is included as Figure S1 in the Supporting Information.

As depicted in Scheme I, the primary step in the reaction of •OH with **Pro** (identified as Step 1) was characterized for all the possible H-atom abstractions by radical attack from both faces of the pyrrolidine ring (i.e., from the side of the carboxylate group or from the opposite one, respectively labeled s and o channels) at C3, C4, and C5 in the side-chain as well as at C2 in the backbone. Two competitive channels of reaction starting from each of the stable carbon-centered radicals (**Pro•**) produced through Step 1 were further explored: the direct addition of •OH to generate **Hyp** (Step 2a) and a second H-atom abstraction from **Pro•** at the different alkyl sites adjacent to each center bearing the unpaired spin (Step 2b) leading to dehydroproline stable species (**Δ-Pro** in Scheme I) previously identified as intermediates in the H-abstraction of **Pro** by radicals, Δ^1-pyrroline-5-carboxylate (**P5C**) in particular.[42,69,70] Once again s and o labeling is used to distinguish among •OH attack to **Pro•** approaching the pyrrolidine ring from the same and opposite side of the carboxylate group, respectively. In closure of a mechanism capable of explaining hydroxyproline formation from **Δ-Pro** intermediates, two final competitive addition processes on the unsaturated C═C moieties were examined as follows: unassisted and assisted water addition eventually leading to production of **Hyp** (Step 3a) and unassisted and assisted •OH addition on the same target sites (Step 3b) eventually leading to distinct **Hyp•** radicals that finally would be able to generate **Hyp** by H-atom reabstraction (Step 3c) from protective species present in the cellular environment such as ascorbate, glutathione, α-tocopherol, carotenoids, and flavonoids.

2.2. Level of Theory. The geometrical structure of each stable species (reactants, products, and prereactive intermediate complexes IC) and transition states (TS) was fully optimized in aqueous solution at the (U)M06/6-31G(d,p) level[71] integrated with the IEF-PCM polarizable continuum model[72−74] without imposing symmetry restrictions and using solute cavities adapted to the molecular shape and constructed with Bondi radii.[75] An ultrafine pruned grid having 99 radial shells and 590 angular points per shell was employed for numerical integration in all M06 calculations to ensure small errors in reaction energies and barriers.[76] Expectation values of the spin operator S^2 were checked to be below 0.76/2.01 for all the open-shell species to ensure minimal spin contamination. The nature of each stationary point was carefully verified by inspection of the eigenvalues of the analytic Hessian in aqueous solution. Thermochemistry was evaluated at 298.15 K relying on the standard treatment for assessing thermal contributions (rigid rotor, harmonic vibrations with no scale factor, etc.) as implemented in the Gaussian09 program.[77] Nonelectrostatic contributions (cavitation, dispersion, and repulsion)[78,79] to the solvent free energy were also evaluated at 298 K. The reaction coordinate associated to each transition state (TS) was inspected by animation of the eigenvector associated to the imaginary frequency. Intrinsic reaction coordinate (IRC) minimum energy reaction paths[80] toward reactants and products were generated with the Hessian-based predictor-corrector (HPC) algorithm[81] including 45 steps for each side with a step size of 2 bohr amu$^{-1/2}$. Representative structures obtained from each side of the reaction path were thus used as the starting point for optimizing the structure of the corresponding intermediate complexes (ICs). UCCSD/cc-pVDZ geometry optimization in aqueous solution was also performed for the species involved in Step 3b which exhibited significant spin contamination at the DFT level. All the calculations were performed using Gaussian09, revision A.1.[77]

3. RESULTS AND DISCUSSION

3.1. First H-Atom Abstraction from Proline by ·OH: Regioselectivity of the Initial Attack. Figure 1 collects the structural features and free energy profiles in aqueous solution at 298.15 K for reactants, TSs, and products for six of the seven reaction channels explored for Step 1, including attack at C3, C4, and C5 from both sides of the pyrrolidine ring (s and o channels). H-abstraction from C2 (not shown) was also characterized for the only possible o-face of attack.

dx.doi.org/10.1021/jp407773u | J. Phys. Chem. B 2014, 118, 37−47

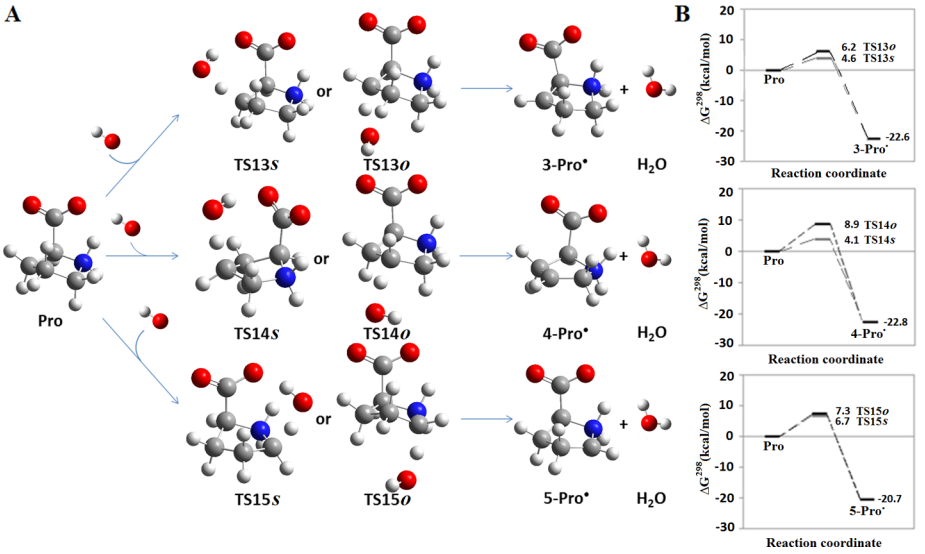

Figure 1. First H-atom abstraction from **Pro** in aqueous solution. (A) Structures for the reactants, TSs, and product radicals, considering both the attack from the carboxyl group side (s-face) and the opposite side of the ring (o-face). Intermediate complexes (IC1s) characterized are not shown here for the sake of clarity; their structures are displayed as Figure S2 in the Supporting Information. (B) Gibbs free energy profiles in aqueous solution relative to reactants for each reaction channel.

As previously anticipated based upon the BDEs values for the forming and breaking of bonds involved in the reaction coordinate for each of these channels, all of them are quite exoergic (and strongly exothermic, see Table S1 in the Supporting Information for the detailed set of data). Side-chain abstraction leading to C3/C4-centered radicals are thermodynamically preferred by ~2 kcal mol^{-1} over H extraction from C2/C5. Activation barriers are in the 4−9 kcal mol^{-1} range, corresponding to the picture of near-diffusion controlled extremely fast processes, even without considering tunneling effects[82,83] typical of this type of reaction. S-face attack is favored over the o-face one in all cases, as the result of differential stabilizing interactions (mainly HB and dipole−dipole alignments) between the approaching •OH and the $-CO_2^-$ moiety in the former plane of approach. Abstraction on C2/C5 ($\Delta G^{\ddagger}$ = 6.9 kcal mol^{-1} for hydrogen removal at C2, not shown in Figure 1) requires surmounting activation barriers 2 kcal mol^{-1} higher with respect to the attack on C3/C4. This kinetic preference toward β/γ channels agrees both with the observed side-chain selectivity and with the reduced site-specificity typical of processes involving highly reactive molecules such as •OH. Whereas thermodynamics mirrors kinetics for s-face H removal (the more exoergic the attack, the lower the barrier height) not a clear trend emerges from the o-face H-abstraction channels, pointing out the relevancy of the interactions established between the carboxylate group and •OH in defining the fate of the process. No basis is found here in support of the assumption that the relative reactivity of the H-abstraction sites in **Pro** would correlate their BDEs ordering, as previously proposed by several authors. Prereactive complexes characterized for these channels are found to be stable in terms of enthalpy relative to reactants by amounts of the order of 7 and 1−2 kcal mol^{-1} for s-attack and o-attack orientations, respectively. Once again this results from differential stabilizing interactions established between •OH and the carboxylate moiety (see the structures of both types of encounter complexes in Figure S2 of the Supporting Information). Unfavorable entropic contributions turn all these prereactive complexes unstable in terms of free energy at 298 K by 1.5−6.6 kcal mol^{-1} (Table S1 of the Supporting Information), providing evidence to discard an eventual role for these intermediate species acting as kinetic traps, a result recently found by Scheiner and Kar[49] for encounter complexes intermediating H-abstraction by •OH from a leucine dipeptide defining the selectivity and specificity of such a H-abstraction.

C-centered **Pro•** radical species obtained as the outcome of Step 1 in zwitterionic form are considerably more stable (20.7−22.8 kcal mol^{-1}, see Figure 1B) than the isolated reactants, with a clear thermodynamic preference toward production of C3/C4 radicals. This fact debilitates in principle the hypothesis previously advanced by several authors[15,61] assuming that **5-Pro•** would be the most stable product for the first H-abstraction. On the other hand, these results are more in line with the conclusions of Nukuna et al.[61] on the preferred reaction sites of **Pro** derived from ^{2}H NMR detection of ^{1}H/^{2}H exchange induced by •OH radicals. The γ(C4)-hydrogen atoms are shown to be more prone to exchange than the δ(C5)-H atoms, which in turn would exchange in a larger extent than the β(C3)-H, whereas α(C2)-H exchange is absent.[61]

Looking for clues to reconcile all these observations, the data collected in Table 1 clearly show an ordering in stability among

Table 1. Relative Stability[a] of the C-Centered Pro• Radicals (Neutral and Zwitterion Hydrogen-Bonded Forms) and Reactivity of the Zwitterionic (zw) Species[b]

	relative ΔG^{298}		hardness (η)
Pro•	neutral	zw	zw
C2	**0.0**	17.0	0.1509
C3	16.7	**16.9**	0.1322
C4	16.5	**16.7**	0.1292
C5	**13.0**	18.7	0.1388

[a]Gibbs free energies calculated at the PCM(water)/UM06/6-31G-(d,p) level and 298.15 K with respect to the most stable C-centered **Pro•** radical isomer, in kilocalories per mole. [b]Hardness was calculated as in the conceptual DFT framework from the energies of the Kohn−Sham frontier orbitals calculated at the same level, in a.u.

dx.doi.org/10.1021/jp407773u | J. Phys. Chem. B 2014, 118, 37−47

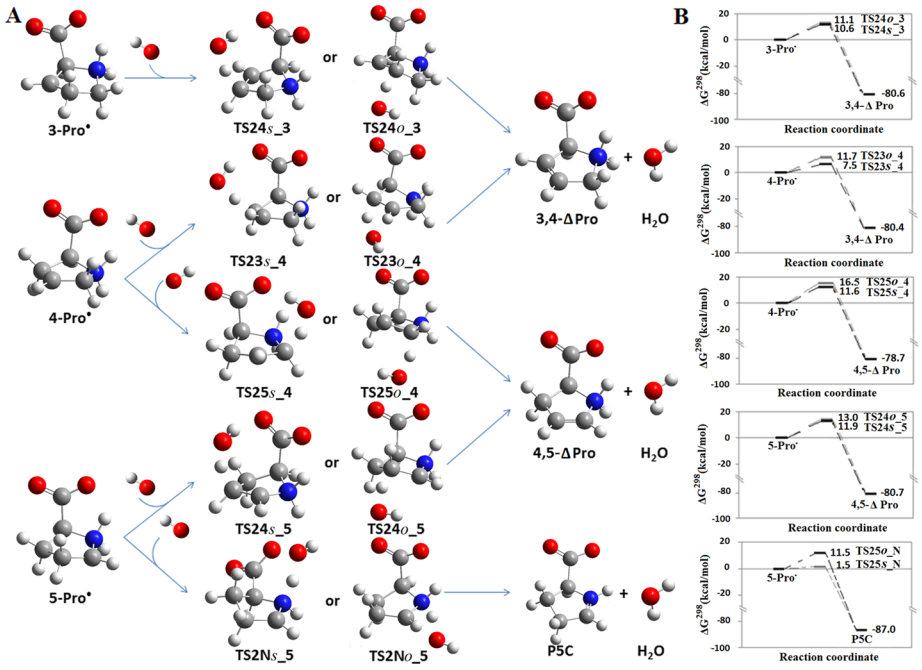

Figure 2. Second H-atom abstraction from **Pro•** C-centered radicals in aqueous solution. (A) Structures for the reactants, TSs, and unsaturated products considering both the attack from the carboxylate side (s-face) and the opposite side of the ring (o-face). Intermediate complexes (IC2s) are not shown here for the sake of clarity; their structures are displayed as Supporting Information in Figure S3. (B) Energetic profiles in aqueous solution are relative to reactants for each of the ten reaction channels considered.

such short-lived open-shell zwitterions that can be significantly altered in passing to the corresponding neutral counterparts through an internal proton transfer that retains the intramolecular HB. Recalling concepts such as the captodative effect[39] and −N(H) lone-pair delocalization in the neutral form makes it possible to explain the differential stabilization of neutral **C2-Pro•** and **C5-Pro•**, which become the most stable radicals in such a form. Variations in pH and ionic strength in environments typical of stressed plants could be influencing the preference among each pair of neutral and zwitterion radical species making difficult a direct comparison of experiments. This could be a key aspect to keep in mind in order to reconcile observations and conclusions coming from different fields.

Concerning further reactivity of these species, in a similar way Gly• and Ala• amino acid radicals produced by •OH attack have been recently shown by Owen et al.[53] to reconvert into their corresponding closed-shell species by H reabstraction from H_2O_2 (involving barriers of ca. 17 kcal mol^{-1}), **Pro•** species might be turned back into **Pro** as follows:

$$\mathbf{Pro}^{\bullet} + H_2O_2 \rightarrow \mathbf{Pro} + HO_2^{\bullet} \quad (1)$$

At physiological pH, the hydroperoxyl radical ($HO_2^{\bullet}$, the weak conjugated acid of $O_2^{\bullet-}$ with a pK_a value of 4.8) obtained as an intermediate in eq 1 is able to promote superoxide dismutation through both spontaneous and superoxide dismutase catalyzed pathways (with respective rate constants of approximately 2×10^5 and 2×10^9 M^{-1} s^{-1})[84] as follows:

$$O_2^{\bullet-} + HO_2^{\bullet} + H^+ \rightarrow H_2O_2 + O_2 \quad (2)$$

acting thus H_2O_2 as a catalyst for the consumption of **Pro•** and $O_2^{\bullet-}$ as shown in eq 3:

$$O_2^{\bullet-} + \mathbf{Pro}^{\bullet} + H^+ \rightarrow \mathbf{Pro} + O_2 \quad (3)$$

Finally, C-centered **Pro•** radicals might also be repaired by H-atom donation from −SH groups or might react with O_2 under aerobic conditions to produce peroxyl radicals that can further dehydrate to yield the expected species hydroxyproline.[42,85]

3.2. Going Further Pro• Radicals: Successive H-Abstraction Routes Leading to Relevant Species Pro Metabolism in Stressed Plants. Our exhaustive search on the triplet and singlet potential energy surfaces in aqueous solution conducted from both sides of attack by •OH over every C-centered radical obtained from Step 1 was unable to locate any TS structure for these processes globally identified as Step 2a in Scheme I. Assisted paths including one and two explicit water molecules acting as catalysts were also explored with the same outcome. In spite of that, as this kind of radical−radical recombination process is expected to display very low barriers and to be strongly exothermic, reaction free-energy values of respectively −85.9, −84.6, and −88.1 kcal mol^{-1} obtained for the favored s-face attacks by •OH over C3, C4, and C5 **Pro•** radicals suggest a first feasible channel leading to **Hyp**.

The goal of transforming the highly reactive C-centered radicals into less deleterious species can also be reached by a successive H-abstraction process from C or N atoms adjacent to the initial radical site, giving place to spontaneous formation of unsaturated cyclic species (Scheme I, Step 2b). Figure 2 collects the structural features and energetic profiles for reactants, TSs, and products (**3,4-Δ-Pro**, **4,5-Δ-Pro**, and **P5C**) for each of the ten reaction channels explored as Step 2b, including •OH attack at adjacent positions from **C3-Pro•**, **C4-Pro•**, and **C5-Pro•** from both faces of approaching the pyrrolidine ring (s and o channels). Taking into account the higher barrier obtained for a first H-abstraction at C2 and the fact that the present study focuses on the search of a possible link between the protective role of proline and the generation of **Hyp**, successive H-abstractions from C2 radical are not further discussed here.

dx.doi.org/10.1021/jp407773u | J. Phys. Chem. B 2014, 118, 37−47

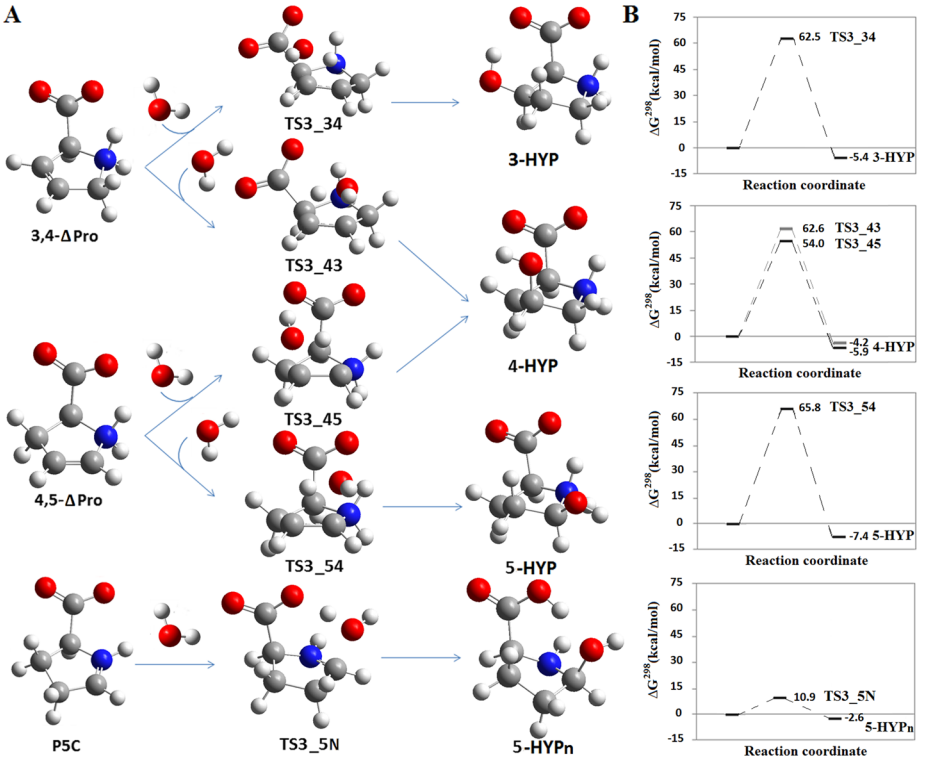

Figure 3. Structure and energetics of the species involved in hydration of **Δ-Pro**. (A) Structure for the reactants and TSs and hydroxyproline isomers (**3-Hyp**, **4-Hyp**, and **5-Hyp**/**Hyp$_n$**) corresponding for the attack from the carboxylate group side of the ring (s-face). Encounter complexes (IC3s) are not shown here for the sake of clarity; their structures are displayed as Supporting Information in Figure S5. (B) Gibbs free energy profiles in aqueous solution at 298.15 K are relative to reactants for each of the five channels explored.

Concerning the prereactive complexes (IC2), those corresponding to the second H-abstraction by •OH approaching from the s-face are fairly more stable than those corresponding to the o-face attack (see details in Figure S3 and Table S1 in the Supporting Information). This is mainly due to •OH··· carboxylate hydrogen-bonding present in all the s-face encounter complexes but in IC2Ns_5. In spite of this observation, and as for IC1 complexes in Step 1, the stabilization gained in forming IC2s is completely overcome by the unfavorable entropic cost of arranging reactants in more organized structures. For this reason all the barrier heights reported in Figure 2B and discussed here correspond to the bimolecular processes, calculated with respect to the reactant separated at the infinite.

The activation barriers obtained for the second H-abstraction are now in the 1.5−16.9 kcal mol^{-1} range, showing a more pronounced variability among different channels. Once again, s-face processes are all favored with respect to the corresponding o-face reaction paths. This remarks the relevance of establishing intermolecular HBs for achieving a differential stabilization of the TSs that leads to reduced heights at the corresponding barriers. Starting from the major products from Step 1 (**4-Pro•** and **3-Pro•**) the kinetically preferred path leads to formation of **3,4-Δ-Pro** with an associated barrier of 7.5 kcal mol^{-1} at 298.15 K in aqueous solution. This value competes well against the mechanistic alternative for converting **Pro•** back to **Pro** under H_2O_2 catalysis (with values of $\Delta G^{\ddagger}$ = 10.7 kcal mol^{-1} and ΔG_{rxn} = −10.9 kcal mol^{-1} for the process of reconverting **4-Pro•**, as the main product from Step 1; see the structure of the species involved in this channel in Figure S4 in the Supporting Information) emerging here as a more favorable channel that enables the envisioning of another feasible route to reach the eventual production of **Hyp** isomers.

Even if obtained as a secondary product from Step 1, a very interesting mechanistic alternative emerges from the **5-Pro•** zwitterion: a successive H abstraction at the N-protonated site produces Δ^1-pyrrolidin-5-carboxylate (**P5C**) through a near-barrierless •OH attack ($\Delta G^{\ddagger}$ = 1.5 kcal mol^{-1}). **P5C** is a well-known precursor in the biosynthesis of proline,[9,86,87] also recently identified by Kenttämaa and co-workers as a product of two consecutive H-abstractions initiated by charged phenyl radicals on this amino acid.[70] Moreover, conversion of **P5C** into **Pro** is known to be efficiently catalyzed by pyrroline 5-carboxylate reductase (**P5CR**, EC 1.5.1.2),[88] an enzyme induced under stress conditions in plants[9,89,90] that consumes one **NADPH** molecule per **P5C** (see Scheme II in Section 3.4).

3.3. Finding the Missing Link toward Hyp: Is It Produced by H_2O/•OH Addition on Δ-Pro? Aiming to find evidence for a plausible mechanistic proposal linking the protective role of proline and the hypothesized production of **5-Hyp** under plant stress, we explored several channels for hydration of **Δ-Pro** species by direct addition of water on the C═C and C═N unsaturation (identified as Step 3a in Scheme I). On the basis of the marked preference toward s-face attacks shown by **Pro** and **Pro•** in Steps 1 and 2b, this face was the only one systematically explored in this case. Figure 3 displays the structural features and energetic profiles for reactants, TSs, and products (**3-Hyp**, **4-Hyp**, and **5-Hyp** zwitterions and neutral species; see explanation below) for each of the five reaction channels explored as Step 3a, resulting from considering both water asymmetric additions on C3═C4 and C4═C5 and a single addition on C5═N.

dx.doi.org/10.1021/jp407773u | J. Phys. Chem. B 2014, 118, 37−47

Scheme II. Feasibility of the Pathways Explored for Assessing Proline Activity As a •OH Scavenger. The Main Reactions Consuming •OH by Both Proline (Pro) and Its Derivatives (Pro•, Δ-Pro/P5C, and Hyp) are Identified by Horizontal and Vertical Blue Labels

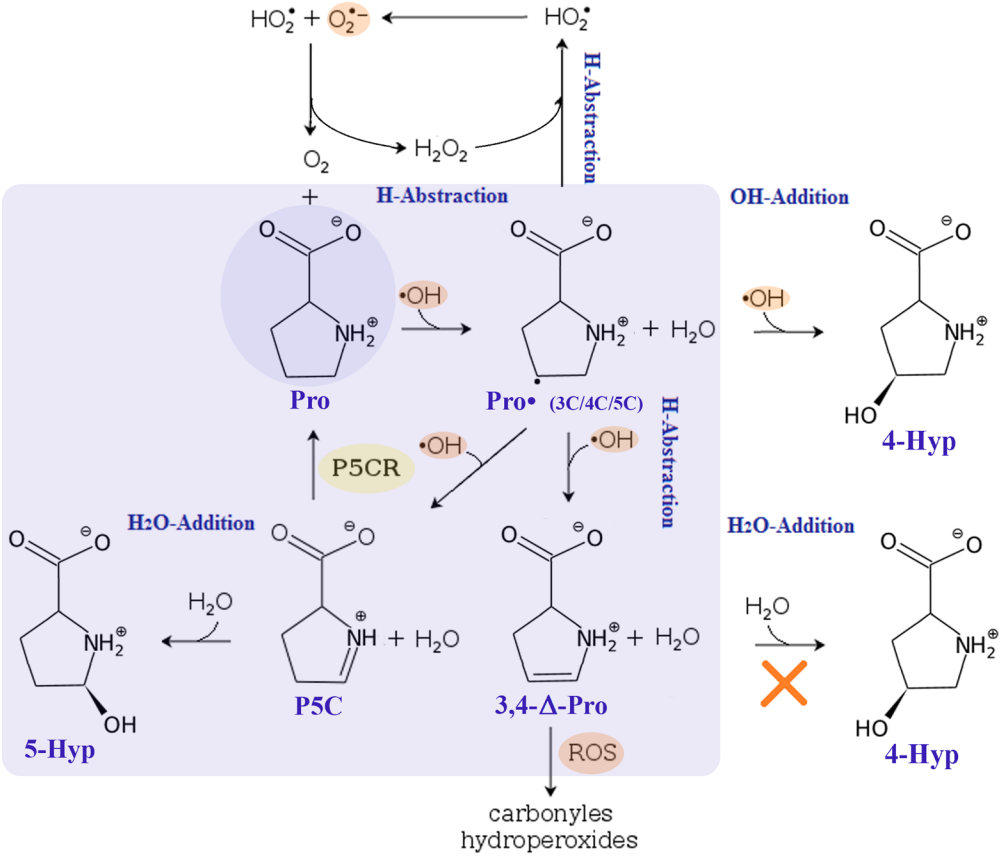

Hydration by direct addition of a water molecule on the C═C bonds is associated to very high barrier heights (ca. 54−66 kcal mol^{-1}), making it possible to discard these reactions as feasible in the absence of a catalyst. On the other hand, direct hydration on the C═N bond in **P5C** appears as a strongly favored reaction channel with a low activation barrier of 10.9 kcal mol^{-1}. This provides the mechanistic missing link we sought for the connection of •OH scavenging by **Pro** with formation of 5-hydroxyproline (**5-Hyp$_n$** in Figure 3A). Notice that in contrast with the rest of the processes studied as Step 3a (for which the zwitterionic form of **Hyp** is the only outcome for direct hydration on both **Δ-Pro** species) 5-hydroxyproline happens to be obtained in the neutral form from this path. A closer inspection on the nature of the reactants, transition states characterized for each hydration channel, and their corresponding IRC reaction paths can be useful to shed light on the differences in the mechanism of each reaction described at a very detailed level.

In the first place, water addition over C═N at **P5C** zwitterion can be depicted as a process assisted by the proximal COO^- moiety acting as a Brönsted base which captures a proton from the approaching H_2O molecule while the emerging hydroxyl anion attacks C5 in a concerted way. This enables the protonated imino moiety to develop a lone pair on N as the reaction proceeds breaking the C═N double bond, while the initial intermolecular hydrogen bond HOH···$^-$O(C═O) evolves to an intramolecular C5-(H)O···HO(C═O) HB as in **5-Hyp$_n$** (see Figure 3A, bottom) once the coupled proton transfer/HO^- addition are completed. Second, concerning the reaction of water on C═C at the different **Δ-Pro** zwitterions, all four channels here characterized (see Figure 3A) correspond to a concerted process, with a water molecule simultaneously attacking the two adjacent C(sp^2) atoms in order to form two new bonds [C(sp^2)···O(H) and C···H] while one H−O bond in H_2O is broken. Reactants and **Hyp** zwitterionic products are thus interconnected, passing through cyclic 4-centered transition state structures, which are quite tensioned and extremely unstable, a fact reflected in the high values obtained for the corresponding barrier heights (see Figure 3B). Taking into account that assistant water molecules acting as bifunctional catalysts have been shown to accelerate hydration and related condensation processes on unsaturated moieties,[91−93] alternative channels including one ancillary water in the reaction coordinate were also explored. Thus, four more relaxed 6-centered cyclic TSs were located, still resulting in associated to noncompetitive barrier heights (50 kcal mol^{-1} or higher, see the last four rows in Table S1 and Figure S6 in the Supporting Information) with respect to hydration of **P5C** linking to **5-Hyp**.

In closing the mechanistic exploration here undertaken, addition of •OH on C═C **Δ-Pro** derivatives (Scheme I, Step 3b) was also examined to assess whether **Hyp** production might be feasible through this alternative pathway as a way of further scavenging •OH. Only a couple of first-order saddle points could be found at the DFT level on the doublet potential energy surface corresponding to the approach of •OH to C3/C5 from the s-face to yield **3-Hyp•**/**5-Hyp•** radicals, and both of them were affected by significant spin contamination (expected values for $S^2 \geq 0.77-0.78$). Considering these structures and their associated energetics untrustworthy, a more rigorous characterization of the

dx.doi.org/10.1021/jp407773u | J. Phys. Chem. B 2014, 118, 37−47

Table 2. Selection of PCM-UM06/6-31G(d,p) Energetics at 298.15 K in Aqueous Solution[a] for the Principal and Secondary Chemical Pathways in the Overall Mechanism of Proline as •OH Scavenger

step and type of reaction	species in the main path	$\Delta G^{\ddagger b}$	$\Delta G_{rxn}{}^{c}$	species in the secondary path	$\Delta G^{\ddagger b}$	$\Delta G_{rxn}{}^{c}$
1: H abstraction	**3-Pro•/4-Pro•**	4.6/4.1	−22.6/−22.8	**5-Pro•**	6.7	−20.7
2a: **Pro•**/•OH assoc.	**3-Hyp$_{zw}$/4-Hyp$_{zw}$**	−[d]	−85.9/−84.6	**5-Hyp$_{zw}$**	−[d]	−88.1
2b: H abstraction	**3,4-Δ-Pro**	7.5	−80.4	**P5C**	1.5	−87.0
3a: hydration	–	–	–	**5-Hyp$_{n}$**	10.9	−2.6

[a]Relative Gibbs free energies calculated at the DFT/PCM level taken with respect to reactants for each step separated to the infinite. [b]Activation barrier height. [c]Reaction free energy. [d]Barrierless radical−radical association processes.

species involved in these two channels was conducted at the PCM(water)/UCCSD/cc-pVDZ level. No first-order saddle points were localized at this level for •OH addition on both C3 and C5. At the same time, it is worth recalling that these **Δ-Pro** derivatives are likely to exert their antioxidant role through interactions of their π-electron density with other ROS such as $^1O_2$ or $O_2^{\bullet-}$, forming carbonyls and hydroperoxides.[40−43,85]

3.4. Overall Mechanism for •OH Scavenging by Proline, Biological Significance in Plant Stress, and a Pro-Pro Cycle Proposal. Key aspects emerging from the extended mechanistic analysis here conducted are summarized in Scheme II. The scheme discriminates among feasible and not feasible reaction channels in a physicochemical and biological context and depicts main structural features of the species interconnected in the •OH scavenging network. A selection of data on energetics for the most relevant channels and intermediates is also collected in Table 2.

The mechanistic evidence collected here based upon DFT/PCM modeling of a network of reaction pathways provides strong support to the concept advanced earlier by Smirnoff and Cumbes[14] on proline having a protective role in stressed plants by acting as a •OH scavenger. This would be accomplished through a complex mechanism which in overview involves consumption of a minimum of two hydroxyl radicals per amino acid molecule and enables the recovery of the original **Pro** by enzymatic recycling of chemically produced **P5C**.

Such an activity would take place in the cellular environment through three main kinds of chemical transformations, including (a) initiation by H-abstraction from **Pro** by •OH with the evidence supporting kinetic and thermodynamic preference toward production of **4-Pro•/3-Pro•** that can be promptly terminated by **Pro•**/•OH radical-pair association, mainly leading to **3-Hyp$_{zw}$/4-Hyp$_{zw}$/5-Hyp$_{zw}$**; (b) a successive H-abstraction step from the intermediate **Pro•** radicals, competitive with termination, with the evidence supporting kinetic and thermodynamic preference toward production of **3,4-Δ-Pro** as a main path, accompanied by a secondary pathway relevant to chemical production of **P5C** passing through **5-Pro•**; and (c) direct hydration of **P5C** to produce **5-Hyp$_{n}$** in competition with enzymatic recycling of **P5C** back to **Pro** as catalyzed by **P5CR/NADPH.**

Through this series of transformations, a molecule of **Pro** would be intrinsically successful in progressively converting deleterious •OH radicals into less-harmful species (**Pro**, **Δ-Pro**, **Hyp$_{zw/n}$**, and water), exerting a protective role in general terms.

To consider all these findings in a proper biological perspective, completing the scenario for an antioxidant activity of proline in stressed plants would require keeping in mind that whereas •OH is one of the most reactive, and thus one of the least selective, radical species with a relatively narrow range of rate constants (k = 10^7−10^{10} M^{-1} s^{-1}) for reacting with amino acids,[85,94] under normal conditions **Pro** is one of the least abundant of them. In a first glance, this might induce one to think that **Pro** would not be the best candidate for exerting an antioxidant activity against •OH. Two more key elements have to be taken into account in composing the picture for sustaining such an activity. The first one is the aforementioned increase in **Pro** concentration experienced by plants under any kind of stress (raising up to 80% of the total pool of amino acids[7−9,15]); the second one is colocalization of both species in the cytosol and chloroplasts, where •OH is commonly produced as a consequence of disruption in the electron transport of photosystems. At these locations **Pro** accumulation reaches, even under nonstressful conditions, concentrations of at least 160 mM,[8,95] becoming considerably more abundant than every other common antioxidant (i.e., 1−5 mM for glutathione and 5−20 mM for ascorbato).[1,2,9] Moreover, cytosol and chloroplasts also are subcellular compartments where **Pro** biosynthesis enzymes such as **P5CR** are localized.[9,96] All these elements provide solid significance to our mechanistic findings in the precise context of proline's accumulation in stressed plants.

Finally, we propose here for the first time a **Pro**-(**P5C**)-**Pro** cycle as depicted in Figure 4, where the efficiency of the

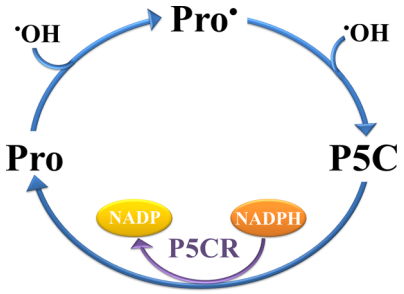

Figure 4. Pro-Pro cycle. Proline captures a first •OH by H-abstraction on C5, followed by a second H-abstraction which also captures •OH, yielding **P5C**. **P5C** is then recycled back to **Pro** by the action of the **P5CR/NADPH** enzymatic system.

enzymatic action exerted by **P5CR** in converting toxic **P5C** back into **Pro**[97] is coupled to the tandem of very fast chemical reactions (in the near-diffusion limit) capturing •OH by **Pro**/**5C-Pro•** to yield **P5C** and two water molecules. As for other enzymes in the biosynthetic pathway of proline, under osmotic stress in which **Pro** accumulation takes place, **P5CR** is also overexpressed[9,90] and **NADPH** is accumulated as a result of inhibition of the Calvin cycle.[98] The enhanced activity of **P5CR** under plant stress will thus extremely favor a prompt recovery of **Pro** from **P5C** originated through chemical scavenging of •OH, acting as a driving force increasing the relevance of this cycle. Although production of **5-Hyp$_{n}$** by **P5C** hydration is characterized here as a very fast chemical process, because toxic **P5C** would be present in very low concentrations by the effect of this cycle, this channel

dx.doi.org/10.1021/jp407773u | J. Phys. Chem. B 2014, 118, 37−47

would yield a very low amount of 5-hydroxyproline, a fact that might explain the lack of experimental evidence of its formation.

4. CONCLUSIONS

Mechanistic evidence was collected here by using DFT/PCM models to sustain a role for proline as a protective $^{\bullet}$OH scavenger under stress in plants. At least two $^{\bullet}$OH radicals are consumed per **Pro** molecule, leading to less deleterious species through strongly exothermic and exergonic channels with very low reaction barriers (mostly in the near-diffusion limit). A clear preference for attacking **Pro** from the carboxylate face (s-face) is noticed, explained by inter- and intramolecular hydrogen-bond interactions that differentially stabilize the corresponding transition states. Our global mechanistic proposal includes two transformation pathways, a main one connecting **Pro** to **3,4-Δ-Pro** through two consecutive H-abstraction processes, the second one in competition with a chance of early termination through barrierless and strongly exothermic radical−radical associative processes leading to **Hyp$_{zw}$**. A secondary path connects to **P5C** as an intermediate capable of evolving to 5-**Hyp$_n$** by hydration, although the action of the **P5CR/NADPH** system (overexpressed under plant stress and colocalized at the same compartment where $^{\bullet}$OH is produced and **Pro** is accumulated) reconverts **P5C** to **Pro**. Such an enzymatic process elicits **P5C** toxicity in the cell, contributing to the reinforcement of **Pro** accumulation and turning hydration leading to **5-Hyp** a quite unlikely channel in photosynthetic tissues. All this evidence gives a solid base for hypothesizing a **Pro**-(**P5C**)-**Pro** cycle, emerging from this study as an original proposal of impact in the field of research in plant stress, whereas consumption of **NADPH** by this cycle would contribute to support a role for **Pro** in maintaining redox homeostasis.

■ ASSOCIATED CONTENT

Ⓢ Supporting Information

Full Gaussian09 reference; differences between neutral and zwitterionic **Pro**; structure of the intermediate complexes for Steps 1, 2b, and 3a; complete table of relative energetics (enthalpy and free energy); structure and energetics for the species involved in reconverting **4C-Pro$^{\bullet}$** to **4C-Pro** by H-abstraction from H_2O_2 and in the water-assisted hydration of **Δ-Pro** species (Step 3a$_w$). This material is available free of charge via the Internet at http://pubs.acs.org.

■ AUTHOR INFORMATION

Corresponding Authors

*E.L.C.: Laboratorio de Química Teórica y Computacional, Instituto de Química Biológica, Facultad de Ciencias, UdelaR, Iguá 4225, Montevideo 11400, Uruguay; e-mail, laurac@fcien.edu.uy; phone, (+598) 2525 2186; fax, (+598) 2525 0749.

*S.S.: Laboratorio de Bioquímica, Depto. de Biología Vegetal, Facultad de Agronomía, UdelaR, Av. E. Garzón 780, CP 12900 Montevideo, Uruguay; e-mail, ssignorelli@fagro.edu.uy; phone, (+598) 2355 3938; fax, (+598) 2356 2037.

Author Contributions

S.S. and E.L.C. designed the strategy of modeling, performed calculations, and interpreted the physicochemical results. S.S., O.B., and J.M. contributed the biological background of the problem. The manuscript was written through contributions of all authors. All authors have given approval to the final version of the manuscript.

Notes

The authors declare no competing financial interest.

■ ACKNOWLEDGMENTS

This work was supported by the uruguayan National Agency of Research and Innovation (ANII, Uruguay; Project FCE_2009_1_2804), CSIC-UdelaR (Project I+D, Group 418), and PEDECIBA. S.S. is very grateful for receiving a graduate bursary granted by ANII (POS_2011_1_3352, M.Sc. in Biology, 2011−2013). The authors are all active members of the National System of Researchers (SNI-ANII, Uruguay).

■ REFERENCES

(1) Mittler, R. Oxidative Stress, Antioxidants and Stress Tolerance. *Trends Plant Sci.* **2002**, *7*, 405−410.

(2) Noctor, G.; Foyer, C. H. Ascorbate and Glutathione: Keeping Active Oxygen under Control. *Annu. Rev. Plant Physiol. Plant Mol. Biol.* **1998**, *49*, 249−279.

(3) Szarka, A.; Tomasskovics, B.; Bánhegyi, G. The Ascorbate-Glutathione-α-Tocopherol Triad in Abiotic Stress Response. *Int. J. Mol. Sci.* **2012**, *13*, 4458−4483.

(4) Halliwell, B.; Gutteridge, J. M. C. *Free Radicals in Biology and Medicine*, 4th ed.; Oxford University Press: Oxford, U.K., 2007.

(5) Zhang, F.; Guo, J.-K.; Yang, Y.-L.; He, W.-L.; Zhang, L.-X. Changes in Pattern of Antioxidant Enzymes in Wheat Exposed to Water Deficit and Rewatering. *Acta Physiol. Plant.* **2004**, *26*, 345−352.

(6) Chen, C.; Dickman, M. B. Proline Suppresses Apoptosis in the Fungal Pathogen *Colletotrichum trifolii*. *Proc. Natl. Acad. Sci. U.S.A.* **2005**, *102*, 3459−3464.

(7) Barnett, N. M.; Naylor, A. W. Amino Acid and Protein Metabolism in Bermuda Grass During Water Stress. *Plant Physiol.* **1966**, *11*, 1222−1230.

(8) Ashraf, M.; Foolad, M. R. Roles of Glycine Betaine and Proline in Improving Plant Abiotic Stress Resistance. *Environ. Exp. Bot.* **2007**, *59*, 206−216M.

(9) Szabados, L.; Savouré, A. Proline: A Multifunctional Amino Acid. *Trends Plant Sci.* **2010**, *15*, 89−97.

(10) Chiang, H.-H.; Dandekar, A. M. Regulation of Proline Accumulation in *Arabidopsis thaliana* (L.) Heynh During Development and in Response to Desiccation. *Plant, Cell Environ.* **1995**, *18*, 1280−1290.

(11) Bray, E. A. Molecular Responses to Water Deficit. *Plant Physiol.* **1993**, *103*, 1035−1040.

(12) Hare, P. D.; Cress, W. A.; van Staden, J. Dissecting the Roles of Osmolyte Accumulation During Stress. *Plant, Cell Environ.* **1998**, *21*, 535−553.

(13) Sharma, S.; Villamor, J. G.; Verslues, P. E. Essential Role of Tissue-Specific Proline Synthesis and Catabolism in Growth and Redox Balance at Low Water Potential. *Plant Physiol.* **2011**, *157*, 292−304.

(14) Smirnoff, N.; Cumbes, Q. J. Hydroxyl Radical Scavenging Activity of Compatible Solutes. *Phytochemistry* **1989**, *28*, 1057−1060.

(15) Matysik, J.; Ali; Bhalu, B.; Mohanty, P. Molecular Mechanisms of Quenching of Reactive Oxygen Species by Proline Under Stress in Plants. *Curr. Sci. India* **2002**, *82*, 525−532.

(16) Alia; Mohanty, P.; Matysik, J. Effect of Proline on the Production of Singlet Oxygen. *Amino Acids* **2001**, *21*, 195−200.

(17) Signorelli, S.; Arellano, J. B.; Melo, T. B.; Borsani, O.; Monza, J. Proline Does Not Quench Singlet Oxygen: Evidence to Reconsider Its Protective Role in Plants. *Plant Physiol. Biochem.* **2013**, *64*, 80−83.

(18) Paleg, L. G.; Stewart, G. R.; Bradbeer, J. W. Proline and Glycine Betaine Influence Protein Solvation. *Plant Physiol.* **1984**, *75*, 974−978.

(19) Samaras, Y.; Bressan, R.; Csonka, M.; García-Ríos, R.; D'Urzo, P.; Rhodes, D. Proline accumulation during drought and salinity. In *Environment and Plant Metabolism: Flexibility and Acclimation*; Smirnoff, N., Ed.; Bios Scientific Publisher: UK, 1995; pp 161−186.

(20) Jain, M.; Mathur, G.; Koul, S.; Sarin, N. B. Ameliorative Effects of Proline on Salt Stress-Induced Lipid Peroxidation in Cell Lines of Groundnut (*Arachis Hypogaea L.*). *Plant Cell Rep.* **2001**, *20*, 463−468.

(21) Hong, Z.; Lakkineni, K.; Zhang, Z.; Verma, D. P. Removal of Feedback Inhibition of Δ^1-Pyrroline-5-Carboxylate Synthetase Results in Increased Proline Accumulation and Protection of Plants from Osmotic Stress. *Plant Physiol.* **2000**, *122*, 1129−1136.
(22) Nanjo, T.; Fujita, M.; Seki, M.; Kato, T.; Tabata, S.; Shinozaki, K. Toxicity of Free Proline Revealed in an *Arabidopsis* T-DNA-Tagged Mutant Deficient in Proline Dehydrogenase. *Plant. Cell Physiol.* **2003**, *44*, 541−548.
(23) Nanjo, T.; Kobayashi, M.; Yoshiba, Y.; Kakubari, Y.; Yamaguchi-Shinozaki, K.; Shinozaki, K. Antisense Suppression of Proline Degradation Improves Tolerance to Freezing and Salinity in *Arabidopsis thaliana*. *FEBS Lett.* **1999**, *461*, 205−210.
(24) Xin, Z.; Browse, J. *eskimo1* Mutants of *Arabidopsis* Are Constitutively Freezing-Tolerant. *Proc. Natl. Acad. Sci. U.S.A.* **1998**, *95*, 7799−7804.
(25) Stepanian, S. G.; Reva, I. D.; Radchenko, E. D.; Adamowicz, L. Conformers of Nonionized Proline. Matrix-Isolation Infrared and Post-Hartree−Fock ab Initio Study. *J. Phys. Chem. A* **2001**, *105*, 10664−10672.
(26) Allen, W. D.; Czinki, E.; Csaszar, A. G. Molecular Structure of Proline. *Chem.—Eur. J.* **2004**, *10*, 4512−4517.
(27) Tian, S. X.; Yang, J. Effects of Intramolecular Hydrogen Bonding on the Ionization Energies of Proline. *Angew. Chem., Int. Ed.* **2006**, *45*, 2069−2072.
(28) Plekan, O.; Feyer, V.; Richter, R.; Coreno, M.; de Simone, M.; Prince, K. C.; Carravetta, V. Investigation of the Amino Acids Glycine, Proline, and Methionine by Photoemission Spectroscopy. *J. Phys. Chem. A* **2007**, *111*, 10998−11005.
(29) Mata, S.; Vaquero, V.; Cabezas, C.; Peña, I.; Pérez, C.; López, J. C.; Alonso, J. L. Observation of Two New Conformers of Neutral Proline. *Phys. Chem. Chem. Phys.* **2009**, *11*, 4141−4144.
(30) Pecul, M.; Ruud, K.; Rizzo, A.; Helgaker, T. Conformational Effects on the Optical Rotation of Alanine and Proline. *J. Phys. Chem. A* **2004**, *108*, 4269−4276.
(31) Cappelli, C.; Monti, S.; Rizzo, A. Effect of the Environment on Vibrational Infrared and Circular Dichroism Spectra of (S)-Proline. *Int. J. Quantum Chem.* **2005**, *104*, 744−757.
(32) Kundrat, M. D.; Autschbach, J. Time Dependent Density Functional Theory Modeling of Chiroptical Properties of Small Amino Acids in Solution. *J. Phys. Chem. A* **2006**, *110*, 4115−4123.
(33) Kapitan, J.; Baumruk, V.; Bouř, P. Demonstration of the Ring Conformation in Polyproline by the Raman Optical Activity. *J. Am. Chem. Soc.* **2006**, *128*, 2438−2443.
(34) Aliev, A. E; Courtier-Murias, D. Conformational Analysis of L-Prolines in Water. *J. Phys. Chem. B* **2007**, *111*, 14034−14042.
(35) Qiu, S.; Li, G.; Wang, P.; Zhou, J.; Feng, Z.; Li, C. pH-Dependent Chirality of L-Proline Studied by Raman Optical Activity and Density Functional Theory Calculation. *J. Phys. Chem. A* **2011**, *115*, 1340−1349.
(36) Zhang, P.; Han, S.; Zhang, Y.; Ford, R. C.; Li, J. Neutron Spectroscopic and Raman Studies of Interaction between Water and Proline. *Chem. Phys.* **2008**, *345*, 196−199.
(37) Contineanu, I.; Neacşu, A.; Zgîrian, R.; Tănăsescu, S.; Perişanu, S. The Standard Enthalpies of Formation of Proline Stereoisomers. *Thermochim. Acta* **2012**, 31−35.
(38) Haasnoot, C. A. G.; De Leeuw, F. A. A. M.; De Leeuw, H. P. M.; Altona, C. Relationship between Proton−Proton NMR Coupling Constants and Substituent Electronegativities. III. Conformational Analysis of Proline Rings in Solution Using a Generalized Karplus Equation. *Biopolymers* **1981**, *20*, 1211−1245.
(39) Viehe, H. G.; Janousek, Z.; Merényi, R.; Stella, L. The Captodative Effect. *Acc. Chem. Res.* **1985**, *18*, 148−154.
(40) Davies, M. J.; Dean, R. T. *Radical-Mediated Protein Oxidation: From Chemistry to Medicine*; Oxford University Press: New York, 1998.
(41) Gosche, M. B.; Chen, Y. H.; Anderson, V. E. Identification of the Sites of Hydroxyl Radical Reaction with Peptides by Hydrogen/Deuterium Exchange: Prevalence of Reactions with the Side Chains. *Biochemistry* **2000**, *39*, 1761−1770.
(42) Xu, G.; Chance, M. R. Hydroxyl Radical-Mediated Modification of Proteins as Probes For Structural Proteomics. *Chem. Rev.* **2007**, *107*, 3514−3543.
(43) Morgan, P. E.; Pattison, D. I.; Davies, M. J. Quantification of Hydroxyl Radical-Derived Oxidation Products in Peptides Containing Glycine, Alanine, Valine, and Proline. *Free Radical Biol. Med.* **2012**, *52*, 328−339.
(44) Lu, H.-F.; Li, F.-Y.; Lin, S. H. Site Specificity of α-H Abstraction Reaction among Secondary Structure Motif-An *Ab Initio* Study. *J. Comput. Chem.* **2007**, *28*, 783−794.
(45) Liessmann, M.; Hansmann, B.; Blachly, P. G.; Francisco, J. S.; Abel, B. Primary Steps in the Reaction of OH Radicals with Amino Acids at Low Temperatures in Laval Nozzle Expansions: Perspectives from Experiment and Theory. *J. Phys. Chem. A* **2009**, *113*, 7570−7575.
(46) Francisco-Márquez, M.; Galano, A. Role of the Sulfur Atom on the Reactivity of Methionine toward OH Radicals: Comparison with Norleucine. *J. Phys. Chem. B* **2009**, *113*, 4947−4952.
(47) Watts, Z. I.; Easton, C. J. Peculiar Stability of Amino Acids and Peptides from a Radical Perspective. *J. Am. Chem. Soc.* **2009**, *131*, 11323−11325.
(48) Doan, H. Q.; Davis, A. C.; Francisco, J. S. Primary Steps in the Reaction of OH Radicals with Peptide Systems: Perspective from a Study of Model Amides. *J. Phys. Chem. A* **2010**, *114*, 5342−5357.
(49) Scheiner, S.; Kar, T. Analysis of the Reactivities of Protein C−H Bonds to H Atom Abstraction by OH Radical. *J. Am. Chem. Soc.* **2010**, *132*, 16450−16459.
(50) Lin, R.-J.; Jang, S.; Wu, C.-C.; Liu, Y.-L.; Li, F.-Y. Site Specificity of OH α-H Abstraction Reaction for a β-Hairpin Peptide: An ab Initio Study. *J. Comput. Chem.* **2011**, *32*, 3409−3422.
(51) Galano, A. Mechanism and Kinetics of the Hydroxyl and Hydroperoxyl Radical Scavenging Activity of *N*-Acetylcysteine Amide. *Theor. Chem. Acc.* **2011**, *130*, 51−60.
(52) Chen, H.-Y.; Jang, S.; Jin, T.-R.; Chang, J.-Y.; Lu, H.-F.; Li, F.-Y. Oxygen Radical-Mediated Oxidation Reactions of an Alanine Peptide Motif. Density Functional Theory and Transition State Theory Study. *Chem. Cent. J.* **2012**, *6*, 33−41.
(53) Owen, M. C.; Szori, M.; Csizmadia, I. G.; Viskolcz, B. Conformation-Dependent OH/H_2O_2 Hydrogen Abstraction Reaction Cycles of Gly and Ala Residues: A Comparative Theoretical Study. *J. Phys. Chem. B* **2012**, *116*, 1143−1154.
(54) Galano, A.; Alvarez-Idaboy, J. R.; Montero, L. A.; Vivier-Bunge, A. OH Hydrogen Abstraction Reactions from Alanine and Glycine: A Quantum Mechanical Approach. *J. Comput. Chem.* **2001**, *22*, 1138−1153.
(55) Galano, A.; Alvarez-Idaboy, J. R.; Cruz-Torres, A.; Ruiz-Santoyo, M .E. Kinetics and Mechanism of the Gas-Phase OH Hydrogen Abstraction Reaction from Methionine: A Quantum Mechanical Approach. *Int. J. Chem. Kinet.* **2003**, *35*, 212−221.
(56) Galano, A.; Alvarez-Idaboy, J. R.; Agacino-Valdés, E.; Ruiz-Santoyo, M. E. Quantum Mechanical Approach to Isoleucine + OH Gas Phase Reaction. Mechanism and Kinetics. *J. Mol. Struct. (Theochem)* **2004**, *676*, 97−103.
(57) Cruz-Torres, A.; Galano, A.; Alvarez-Idaboy, J. R. Kinetics and Mechanism of the β-Alanine + OH Gas Phase Reaction: A Quantum Mechanical Approach. *Phys. Chem. Chem. Phys.* **2006**, *8*, 285−292.
(58) Masuda, T.; Nakano, S.; Kondo, M. Rate Constants for the Reactions of OH Radicals with the Enzyme Proteins as Determined by the p-Nitrosodimethylaniline Method. *J. Radiat. Res.* **1973**, *14*, 339−345J.
(59) Pruetz, W. A.; Vogel, S. Specific Rate Constants of Hydroxyl Radical and Hydrated Electron Reactions Determined by the RCL Method. *Z. Naturforsch., B* **1976**, *31B*, 1501−1510.
(60) Rustgi, S.; Joshi, A.; Moss, H.; Riesz, P. ESR of Spin-Trapped Radicals in Aqueous Solutions of Amino Acids: Reactions of the Hydroxyl Radical. *Int. J. Radiat. Biol.* **1977**, *31*, 415−440.
(61) Nukuna, B. N.; Goshe, M. B.; Anderson, V. E. Sites of Hydroxyl Radical Reaction with Amino Acids Identified by ^{2}H NMR Detection of Induced ^{1}H/^{2}H Exchange. *J. Am. Chem. Soc.* **2001**, *123*, 1208−1214.

(62) Štefanić, I.; Bonifacic, M.; Asmus, K.-D.; Armstrong, D. A. Absolute Rate Constants and Yields of Transients from Hydroxyl Radical and H Atom Attack on Glycine and Methyl-Substituted Glycine Anions. *J. Phys. Chem. A* **2001**, *105*, 8681−8690.
(63) Galano, A.; Cruz-Torres, A. OH Radical Reactions with Phenylalanine in Free and Peptide Forms. *Org. Biomol. Chem.* **2008**, *6*, 732−738.
(64) Lin, R.-J.; Wu, C.-C.; Jang, S.; Li, F.-Y. Variation of Reaction Dynamics for OH Hydrogen Abstraction from Glycine between *Ab Initio* Levels of Theory. *J. Mol. Model.* **2010**, *16*, 175−182.
(65) O'Reilly, R. J.; Chan, B.; Taylor, M. S.; Ivanic, S.; Bacskay, G. B.; Easton, C. J.; Radom, L. Hydrogen Abstraction by Chlorine Atom from Amino Acids: Remarkable Influence of Polar Effects in Regioselectivity. *J. Am. Chem. Soc.* **2011**, *133*, 16553−16559.
(66) Berkowitz, J.; Ellison, G. B.; Gutman, D. Three Methods to Measure RH Bond Energies. *J. Phys. Chem.* **1994**, *98*, 2744−2765.
(67) Luo, Y.-R. *Comprehensive Handbook of Chemical Bond Energies*; CRC Press: Boca Raton, FL, 2007.
(68) Moore, B. N.; Julian, R. R. Dissociation Energies of X-H Bonds in Amino Acids. *Phys. Chem. Chem. Phys.* **2012**, *14*, 3148−3154.
(69) Ly, T.; Julian, R. R. Residue-Specific Radical-Directed Dissociation of Whole Proteins in Gas Phase. *J. Am. Chem. Soc.* **2008**, *130*, 351−358.
(70) Pates, G. O.; Guler, L.; Nash, J. J.; Kenttämaa, H. I. Reactivity and Selectivity of Charged Phenyl Radicals toward Amino Acids in a Fourier Transform Ion Cyclotron Resonance Mass Spectrometer. *J. Am. Chem. Soc.* **2011**, *133*, 9331−9342.
(71) Zhao, Y.; Truhlar, D. G. Density Functionals with Broad Applicability in Chemistry. *Acc. Chem. Res.* **2008**, *41*, 157−167.
(72) Miertuš, S.; Tomasi, J. Approximate Evaluations of the Electrostatic Free Energy and Internal Energy Changes in Solution Processes. *Chem. Phys.* **1982**, *65*, 239−245.
(73) Cancès, E.; Mennucci, B.; Tomasi, J. A New Integral Equation Formalism for the Polarizable Continuum Model: Theoretical Background and Applications to Isotropic and Anistropic Dielectrics. *J. Chem. Phys.* **1997**, *107*, 3032−3041.
(74) Tomasi, J. Selected Features of the Polarizable Continuum Model for the Representation of Solvation. *Wiley Interdiscip. Rev.: Comput. Mol. Sci.* **2011**, *1*, 855−867.
(75) Bondi, A. Van der Waals Volumes and Radii. *J. Phys. Chem.* **1964**, *68*, 441−452.
(76) Wheeler, S. E.; Houk, K. N. Integration Grid Errors for Meta-GGA-Predicted Reaction Energies: Origin of Grid Errors for the M06 Suite of Functionals. *J. Chem. Theory Comput.* **2010**, *6*, 395−404.
(77) Frisch, M. J.; Trucks, G. W.; Schlegel, H. B. et al., Gaussian 09, Rev. A.1; Gaussian Inc.: Wallingford, CT, 2009. See the complete reference in the Supporting Information.
(78) Floris, F.; Tomasi, J.; Pascual-Ahuir, J. L. Dispersion and Repulsion Contributions to the Solvation Energy: Refinements to a Simple Computational Model in the Continuum Approximation. *J. Comput. Chem.* **1991**, *12*, 784−791.
(79) Floris, F.; Tomasi, J. Evaluation of the Dispersion Contribution to the Solvation Energy. A Simple Computational Model in the Continuum Approximation. *J. Comput. Chem.* **1989**, *10*, 616−627.
(80) Fukui, K. The Path of Chemical Reactions—The IRC Approach. *Acc. Chem. Res.* **1981**, *14*, 363−368.
(81) Hratchian, H. P.; Schlegel, H. B. Accurate reaction paths using a Hessian based predictor-corrector integrator. *J. Chem. Phys.* **2004**, *120*, 9918−9924.
(82) Truhlar, D. G. Tunneling in enzymatic and nonenzymatic hydrogen transfer reactions. *J. Phys. Org. Chem.* **2010**, *23*, 660−676.
(83) Kuznetsov, A. M.; Ulstrup, J. Proton and Hydrogen Atom Tunneling in Hydrolytic and Redox Enzyme Catalysis. *Can. J. Chem.* **1999**, *77*, 1085−1096.
(84) Fridovich, I. Superoxide Dismutases. *Annu. Rev. Biochem.* **1975**, *44*, 147−159.
(85) Davies, M. J. The Oxidative Environment and Protein Damage. *Biochem. Biophys. Acta* **2005**, *1703*, 93−109.
(86) Hu, C. A.; Delauney, A. J.; Verma, D. P. A Bifunctional Enzyme (Δ^1-Pyrroline-5-Carboxylate Synthetase) Catalyzes the First Two Steps in Proline Biosynthesis in Plants. *Proc. Natl. Acad. Sci. U.S.A.* **1992**, *89*, 9354−9358.
(87) Delauney, A.; Verma, D. P. S. Proline biosynthesis and osmoregulation in plants. *Plant J.* **1993**, *4*, 215−223.
(88) Delauney, A.; Verma, D. P. S. A soybean gene encoding Δ^1-pyrroline-5-carboxylate reductase was isolated by functional complementation in *Escherichia coli* and is found to be osmoregulated. *Mol. Gen. Genet.* **1990**, *221*, 299−305.
(89) Verbruggen, N.; Villarroel, R.; Van Montagu, M. Osmoregulation of a Pyrroline-5-Carboxylate Reductase Gene in *Arabidopsis thaliana*. *Plant Physiol.* **1993**, *103*, 771−781.
(90) Mattioni, C.; Lacerenza, N .G.; Troccoli, A.; De Leonardis, A. M.; Di Fonzo, N. Water and Salt Stress-Induced Alterations in Proline Metabolism of Triticum Durum Seedlings. *Physiol. Plant.* **1997**, *101*, 787−792.
(91) Coitiño, E. L.; Tomasi, J.; Ventura, O. N. Importance of Water in Aldol Condensation Reactions of Acetaldehyde. *J. Chem. Soc., Faraday Trans.* **1994**, *90*, 1745−1755.
(92) Nguyen, M. T.; Matus, M. H.; Jackson, V. E.; Vu, T. N.; Rustad, J. R.; Dixon, D. A. Mechanism of the Hydration of Carbon Dioxide: Direct Participation of H_2O versus Microsolvation. *J. Phys. Chem. A* **2008**, *112*, 10386−10398.
(93) Sun, X.-M.; Wei, X.-G.; Wu, X.-P.; Ren, Y.; Wong, N.-B.; Li, W.-K. Cooperative Effect of Solvent in the Neutral Hydration of Ketenimine: An *Ab Initio* Study Using the Hybrid Cluster/Continuum Model. *J. Phys. Chem. A* **2010**, *114*, 595−602.
(94) Buxton, G. V.; Greenstock, C. L.; Helman, W. P.; Ross, A. B. Critical-Review of Rate Constants for Reactions of Hydrated Electrons, Hydrogen-Atoms and Hydroxyl Radicals ($^{\bullet}OH/^{\bullet}O^{-}$) in Aqueous Solution. *J. Phys. Chem. Ref. Data* **1988**, *17*, 513−886.
(95) Büssis, D.; Heineke, D. Acclimation of Potato Plants to Polyethylene Glycol-Induced Water Deficit. II. Contents and Subcellular Distribution of Organic Solutes. *J. Exp. Bot.* **1998**, *49*, 1361−1370.
(96) Szoke, A.; Miao, G. H.; Hong, Z.; Verma, D. P. S. Subcellular location of Δ-pyrroline-5-carboxylate reductase in root/nodule and leaf of soybean. *Plant Physiol.* **1992**, *99*, 1642−1649.
(97) Miller, G.; Honig, A.; Stein, H.; Susuki, N.; Mittler, R.; Zilberstein, A. Unraveling Δ^1-Pyrroline-5-Carboxylate (P5C)/Proline Cycle in Plants by Uncoupled Expression of Proline Oxidation Enzymes. *J. Biol. Chem.* **2009**, *284*, 26482−26492.
(98) Long, S. P; Humphires, S.; Falkowski, P. G. Photoinhibition of Photosynthesis in Nature. *Annu. Rev. Plant Physiol.* **1994**, *45*, 633−662.